Electronic Supplementary Material (ESI) for Environmental Science: Nano.

Potentially aerosolized nanoparticles in road dust from Shanghai: Distribution, identification, and environmental implications

Yi Yang[†§*], Marina Vance [‡], Feiyun Tou [†], Andrea Tiwari[‡], Min Liu[†], Michael F. Hochella, Jr.[§#]

[†]Key Laboratory of Geographic Information Science of the Ministry of Education, Shanghai Key lab for Urban Ecological Processes and Eco-Restoration, East China Normal University, 3663 North Zhongshan Road, Shanghai, 200062, China

[‡]Center for Sustainable Nanotechnology, Institute for Critical Technology and Applied Science, Virginia Tech, Blacksburg, VA 24061, USA

[§]The Center for NanoBioEarth, Department of Geosciences, Virginia Tech, Blacksburg, VA 24061, USA

[#]Geosciences Group, Energy and Environment Directorate, Pacific Northwest National Laboratory, Richland, WA 99352, USA

- Supplemental information -

Contents:

1. Description of sampling sites

Table S1. Description of sampling sites

Sampling site	Location	Latitude (°N)	Longitude (°E)	Sites ambient environment

1	Minhang	31°00′45″	121°19′39″	heavy traffic density road (mainly are diesel-powered trucks)
2	Jinshan	30°51′54″	121°17′44″	rural road, close to farmland
3	Jinshan	30°52′19″	121°08′15″	heavy traffic density road in an industrial area
4	Jinshan	30°48′01″	121°10′52″	within the range of a petrochemical industrial area
5	Jinshan	30°47′47″	121°15′42″	scarce traffic, sparsely populated area, near an e-waste plant
6	Jinshan	30°43′29″	121°17′40″	within the range of a petrochemical industrial area
7	Jinshan	30°42′37″	121°17′27″	within the range of a petrochemical industrial area
8	Jinshan	30°43′50″	121°21′57″	near a high-speed rail train station
9	Jinshan	30°45′51″	121°23′45″	scarce traffic, sparsely populated area, next to a power plant
10	Fengxian	30°51′14″	121°30′08″	rural road, close to farmers' house
11	Fengxian	30°51′08″	121°31′14″	industrial area, adjacent to many factories' warehouses
12	Fengxian	31°00′31″	121°30′02″	rural road
13	Pudong	31°01′44″	121°34′13″	in a residential area
14	Fengxian	30°56′36″	121°35′34″	rural road, close to farmers' house
15	Pudong	30°53′55″	121°54′58″	a remote, scarce traffic, sparsely populated area
16	Pudong	30°56′52″	121°48′06″	rural road, close to farmlands
17	Pudong	31°00′54″	121°45′12″	near an airport area
18	Pudong	31°06′34″	121°42′19″	rural road
19	Pudong	31°09′40″	121°47′33″	near an airport area
20	Pudong	31°14′45″	121°42′15″	in a high-tech industrial park
21	Pudong	31°14′52″	121°36′23″	in a manufacturing industrial park
22	Minhang	31°05′29″	121°29′52″	close to a heat & power plant, heavy traffic density road
23	Pudong	31°10′56″	121°29′31″	next to the Shanghai World Expo site
24	Pudong	31°11′48″	121°35′37″	in university campus, next to a library
25	Pudong	31°13′17″	121°32′13″	heavy traffic density, prosperous and densely populated area
26	Pudong	31°14′09″	121°30′21″	in the center of CBD
27	Pudong	31°16′37″	121°34′45″	near a residential area
28	Pudong	31°20′24″	121°37′19″	heavy traffic density in a free trade zone, mainly are trucks
29	Pudong	31°22′08″	121°30′12″	near a large-scale sand mining ship factory
30	Baoshan	31°24′39″	121°29′17″	in a green/park area within the range of a steel plant
31	Baoshan	31°21′47″	121°25′55″	near a residential area
32	Yangpu	31°20′18″	121°30′25″	outside the gate of a university campus
33	Yangpu	31°18′18″	121°30′37″	in a densely populated and busy cars commercial district
34	Songjiang	31°06′29″	121°10′34″	within a national forest park area
35	Songjiang	31°05′30″	121°11′35″	within a national forest park area
36	Songjiang	31°02′56″	121°12′27″	in university campus
37	Songjiang	30°59′55″	121°02′34″	heavy traffic density road (mainly are buses, automobiles)
38	Jiading	31°18′17″	121°10′11″	near a civic square, scarce traffic
39	Jiading	31°21′18″	121°13′37″	scarce traffic, sparsely populated area
40	Jiading	31°26′54″	121°16′12″	heavy traffic density road (mainly are diesel-powered trucks)

41	Baoshan	31°28′17″	121°19′25″	heavy traffic density road, near the exit of highway toll station
42	Baoshan	31°27′25″	121°24′38″	highly polluted area by a power plant, busy traffic
43	Zhabei	31°18′52″	121°23′22″	in university campus, next to teaching buildings
44	Yangpu	31°16′60″	121°32′10″	in a green/park area
45	Hongkou	31°15′34″	121°30′35″	close to an open green square
46	Xuhui	31°11′48″	121°26′00″	in a densely populated and busy cars commercial district
47	Xuhui	31°09′21″	121°25′20″	near Shanghai south railway station
48	Zhabei	31°14′39″	121°27′06″	next to Shanghai railway station, busy flow of people and cars
49	Putuo	31°13′55″	121°23′56″	in university campus
50	Putuo	31°17′15″	121°20′17″	in a green/park area
51	Yangpu	31°17′11″	121°29′51″	in university campus; a heavy traffic area where the inner ring viaduct passes by
52	Huangpu	31°12′32″	121°27′27″	in a shopping street close to a stadium
53	Huangpu	31°14′02″	121°28′00″	People's Square where having densely people and cars, commercial area
54	Minhang	31°10′36″	121°25′00″	in a high-tech industrial park
55	Yangpu	31°15′07″	121°29′45″	commercial/residential buildings along both sides of road
56	Jing'an	31°13′25″	121°26′33″	in a densely populated and busy cars commercial district
57	Zhabei	31°17′47″	121°25′57″	in a high-tech industrial park
58	Minhang	31°02′57″	121°28′20″	close to a heat & power plant, heavy traffic density road, chemical engineering area
59	Xuhui	31°07′28″	121°27′43″	near an entrance of overpass
60	Minhang	31°13′16″	121°19′40″	in a green/park area，outside is a shopping and snack street
61	Minhang	31°09′21″	121°21′17″	near a residential area
62	Changning	31°11′30″	121°21′33″	heavy traffic density near Shanghai zoo
63	Yangpu	31°18′58″	121°31′50″	in a green/park area
64	Huangpu	31°11′37″	121°28′02″	near an entrance of underground tunnel, heavy traffic density
65	Hongkou	31°16′26″	121°28′45″	next to Shanghai football stadium, busy traffic volume
66	Putuo	31°16′38″	121°26′10″	in a green/park area

2. Detection limits of trace elements

Detection limit (DL) of each analyzed trace element is listed in Table S2.

Table S2. Detection limits (DL) of trace elements (μg/L)

	DL (μg/L)		DL (μg/L)
V	0.23	Zn	0.38
Cr	0.1	As	0.07
Fe	0.79	Sr	0.24
Mn	0.05	Mo	0.72
Co	0.04	Sn	0.24

Ni	0.1	Ba	0.92
Cu	0.19	Pb	1

3. Description of the dust aerosolization methods

Inlet air was conditioned using a hydrocarbon trap and a high efficiency particulate air (HEPA) filter to a particle concentration <5 cm^{-3} and passed through a mass flow controller prior to entering the disperser.

Following aerosolization, samples were passed through a PM2.5 cyclone (URG-2000-30EN, URG Corp.) to eliminate larger particles and directed to one of three sampling trains:

- Using sampling train A, aerosolized dust was drawn onto pre-weighed 47 mm Teflon filters (JAWP04700, Millipore) using an air sampling pump operating at 9 L min^{-1} (Leland Legacy, SKC Corp). The filters were pre-cleaned by soaking in 10% HNO_3 overnight. Filters were digested and analyzed for metal concentrations. (66 samples)
- Using sampling train B, particles were drawn at 1 L min^{-1} through a Microanalysis Particle Sampler (California Measurements) with 200-mesh copper TEM grids with lacey carbon support film (Electron Microscopy Sciences) affixed to the second and third collection stages (D_{50} cutoff points of 300 nm and 50 nm, respectively). (Selected 9 samples, including sample 5, 7, 26, 42, 47, 48, 51, 53 and 66)
- Using sampling train C, aerosolized dust was directed into a 520 L polyethylene chamber (AtmosBag, Sigma Aldrich) filled with particle-scrubbed air (<5 cm^{-3}) to allow sufficient time for the aerosol sizing instruments to collect data. Aerosol size distributions were measured using a Scanning Mobility Particle Sizer and an Aerodynamic Particle Sizer (3936NL and 3321, TSI) operated in 4-min scans. Resulting size datasets were merged using DataMerge (TSI) to produce one size distribution spanning 10 nm – 20 µm. Following each dispersion, the chamber was evacuated and refilled until a background aerosol number concentration was ≤ 10 # cm^{-3} (average 2.4 ± 1.0 # cm^{-3} in this study). (Selected 12 samples, including 5, 7, 9, 13, 26, 35, 42, 47, 48, 51, 53, 66)

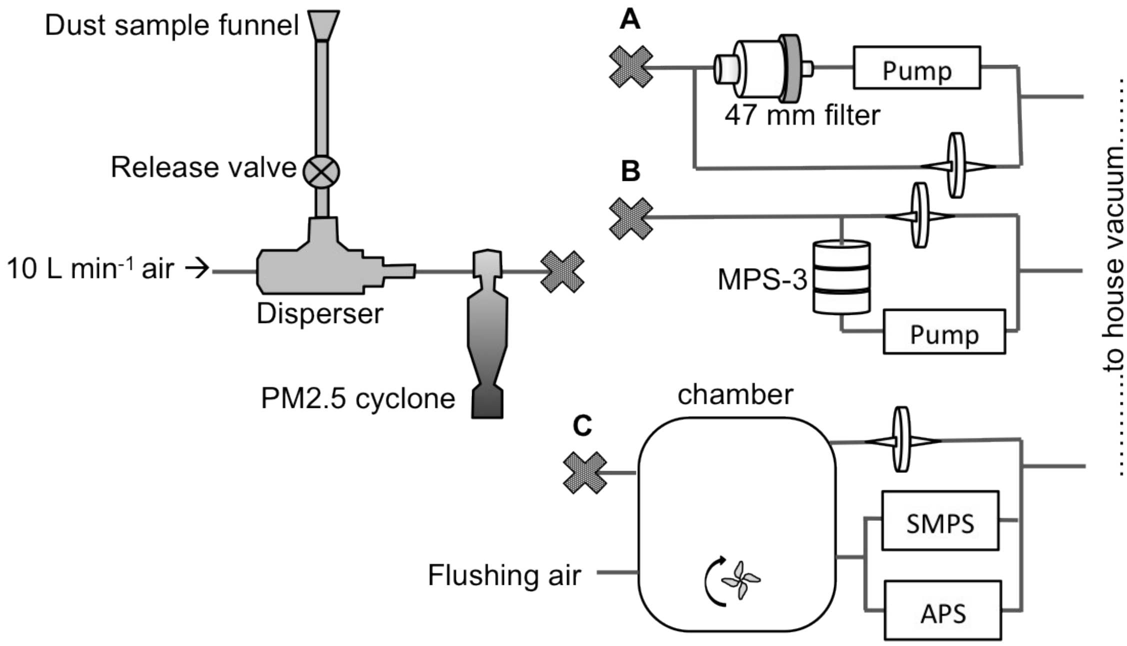

Fig. S1 Aerosolization system. Only one sampling train was employed at a time, attached at the "X" on the aerosol generation system. Because the disperser generates an instantaneous puff of aerosols, each sample was collected on the filter and MPS-3 for 10 seconds. SMPS/APS samples were measured for operated for approximately 10 seconds for each sample. Aerosolized dust in the excess flow was captured using a vent filter. The disperser apparatus and cyclone were cleaned between dispersions by sonication in ultrapure water and air drying.

Quality assurance and quality control (QA/QC): All bulk dust samples were aerosolized in duplicate and further analyzed by ICP-MS for metal concentration. The relative standard deviation (RSD) values for each metal concentration was less than 22%. After each aerosolization procedure, the whole aerosolization system was disassembled, air flushed and cleaned in Milli-Q water by ultrasonic bath. Blank controls were tested for background contamination from the aerosolization system and no/negligible target metal contamination was detected from the blank controls in our experiments. The RSD value was less than 30% for the peak measurement of all size distributions, which further attests to the repeatability of the aerosolization technique used in this study

4. Metal concentrations and distribution in bulk dust

The concentrations of heavy metals in Shanghai street dust samples are shown in Fig. S2. Iron concentrations were in the range of 14,000-150,000 mg kg^{-1} with the average of 30,745 mg kg^{-1}, which is 1-6 orders of magnitude higher than other metals. Mn, Zn and Ba followed with average concentrations of 768, 716 and 538 mg kg^{-1}, respectively. It is noticeable that lead concentrations ranged from 18.5 to 3192 mg kg^{-1} with an average of 213 mg kg^{-1}. Sr and Cu had average concentrations of 189 and 134 mg kg^{-1}, respectively.

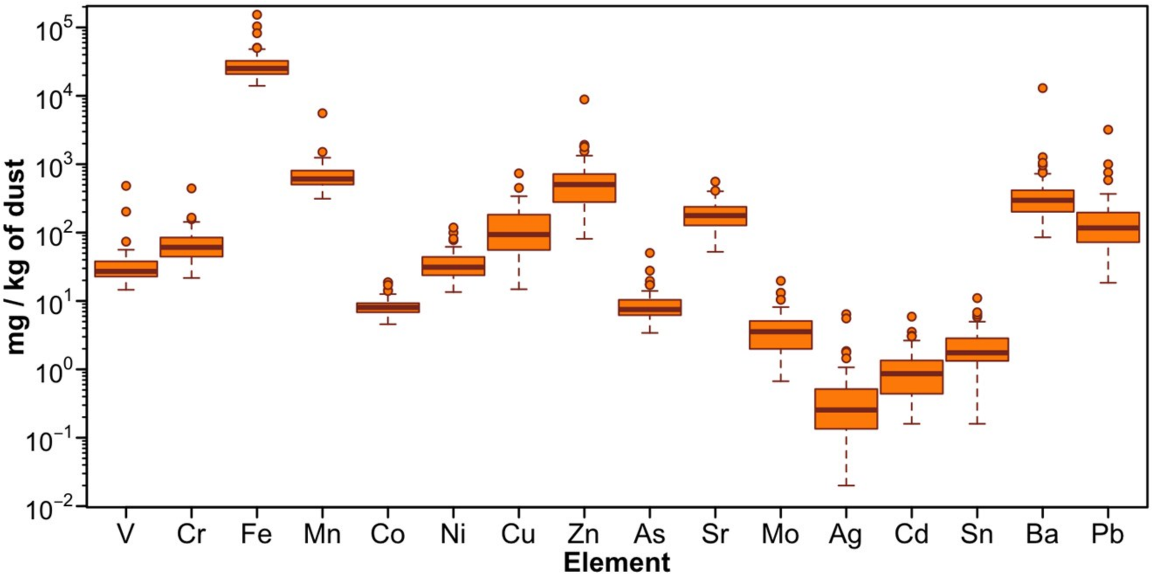

Fig. S2 Concentrations of heavy metals in bulk street dust samples from Shanghai

Spatial distributions of metals, including V, Cr, Fe, Mn, Co, Ni, Cu, Zn, As, Cd, Sn, Ba and Pb were generated using GIS. As shown in Supplementary Fig. S3 online, there is a generally similar distribution pattern for metals in Shanghai. The spots with relatively elevated concentrations were found not only in the downtown area, but also in the northern and southern areas where the Jinshan, Baoshan, and Pudong districts are located.

The highest concentrations of V, Cr and Mn were found in site 42, nearby a coal power plant in the Baoshan district. Site 51, which had the highest concentrations of Fe, Co, Zn and Ba was located on a downtown campus, in a heavy traffic area near the inner ring viaduct. The highest Cu and As concentrations were found in site 58, located near the Minhang powerplant and a number of chemical plants. The highest concentration of Cd was found in site 53, near a downtown commercial center. Sites 5, 6 and 7 were located in the Jinshan district, where there is a petrochemical industry area, and were elevated concentrations of Ni, Mo and Pb were found. The highest concentration of lead (3192 mg kg^{-1}) was measured in site 5, near an electronics waste (e-waste) recycling plant.

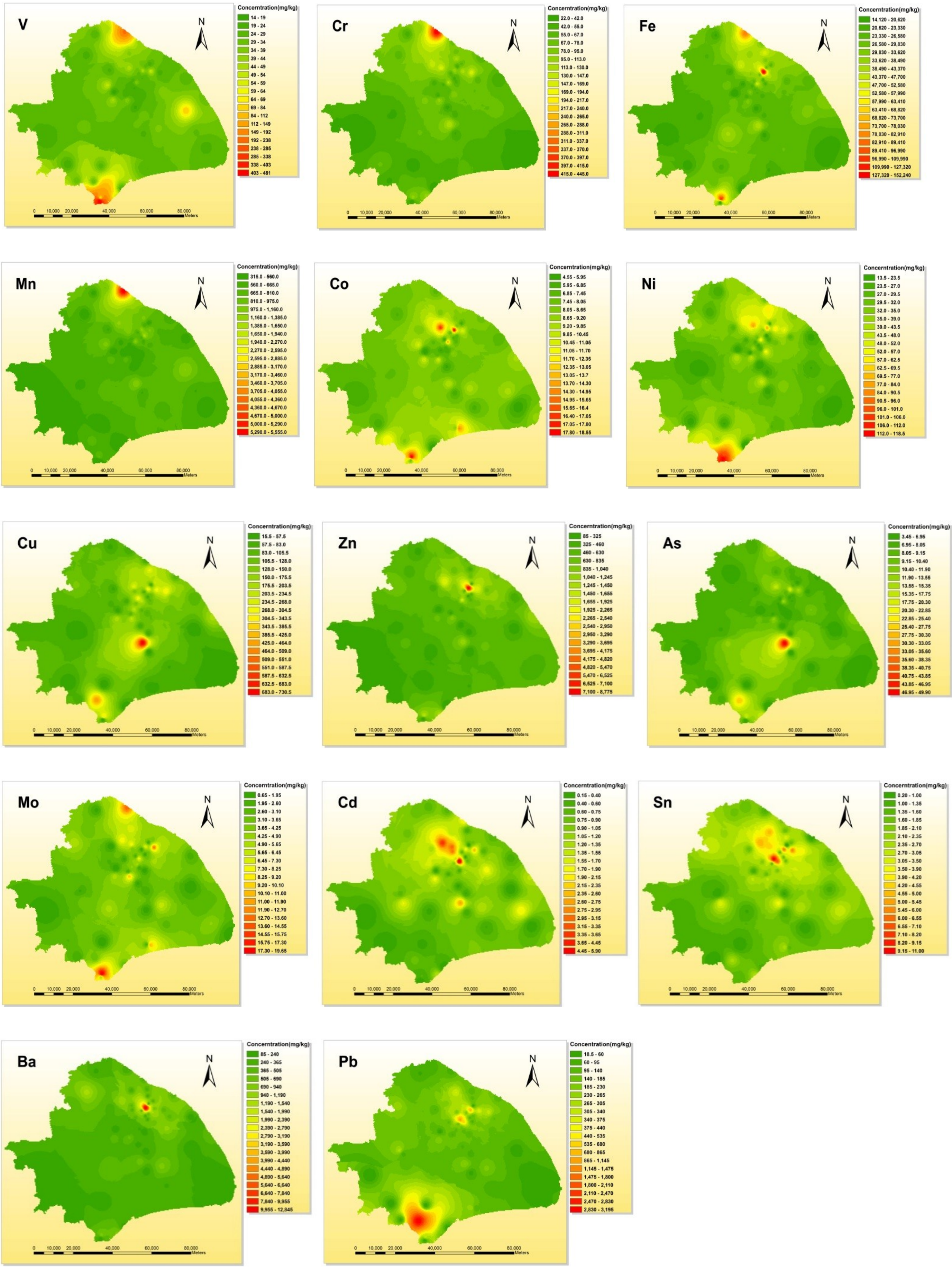

Fig. S3 GIS maps of metals in bulk dust in Shanghai.

5. Grain size distribution in bulk dust

The grain size distribution of bulk samples were measured using a laser diffraction particle size analyzer (LS13320, Berckman). Results showed that the PM2.5 fraction represented 4-18 % of the total volume of bulk dust with an average contribution of 9% (Supplementary Fig. S4 online). Additionally, PM2.5 represented more than 10% of the total dust volume in 30% of samples, which is a significant amount considering the small volume that individual PM2.5 particles contribute to overall dust samples. Although the volume contribution of PM2.5 to the total dust is lower than all other measured fractions, this size range is of particular significance for its environmental and health-related implications.

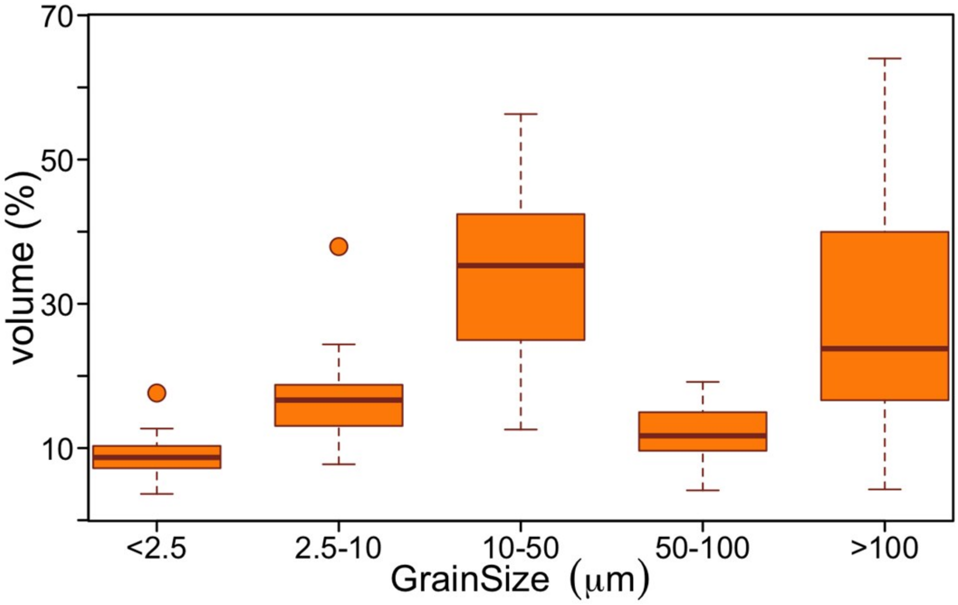

Fig S4 Size distribution of bulk dust samples in Shanghai.

6. Metal concentrations and distribution in aerosolized dust samples

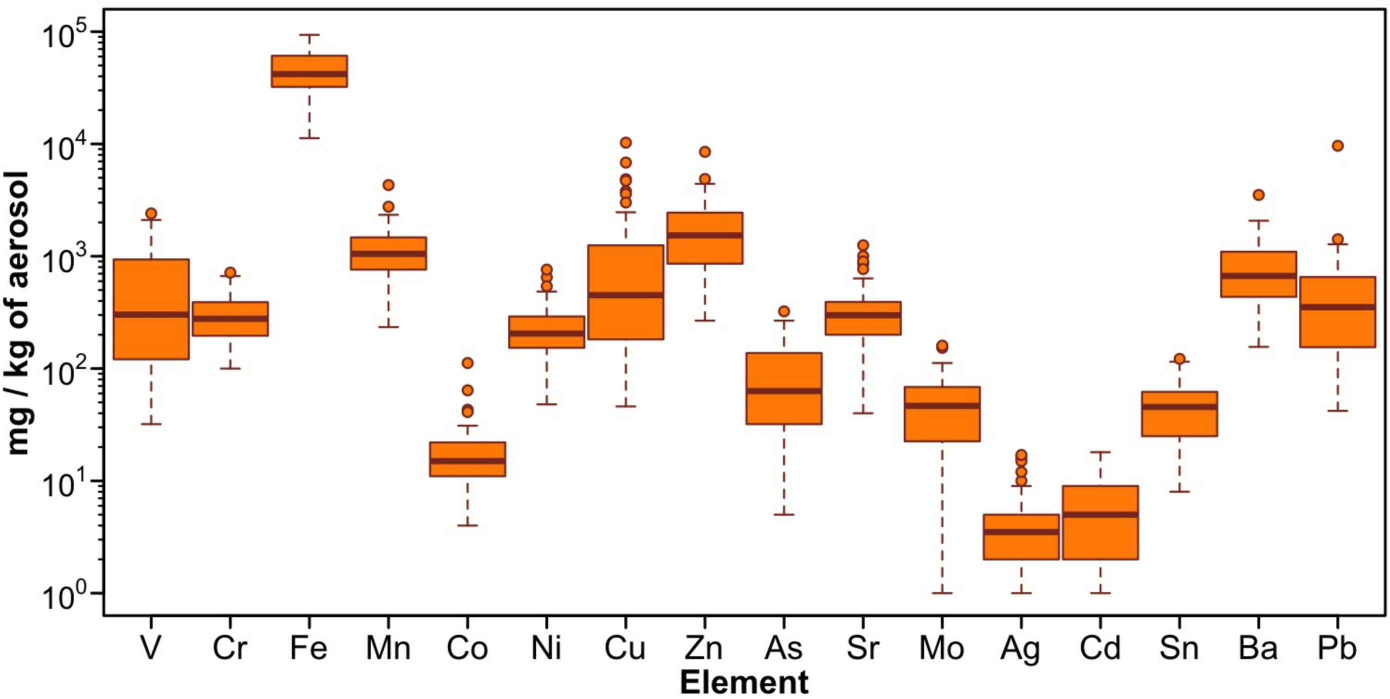

Fig. S5 Metal concentrations in all aerosolized dust samples

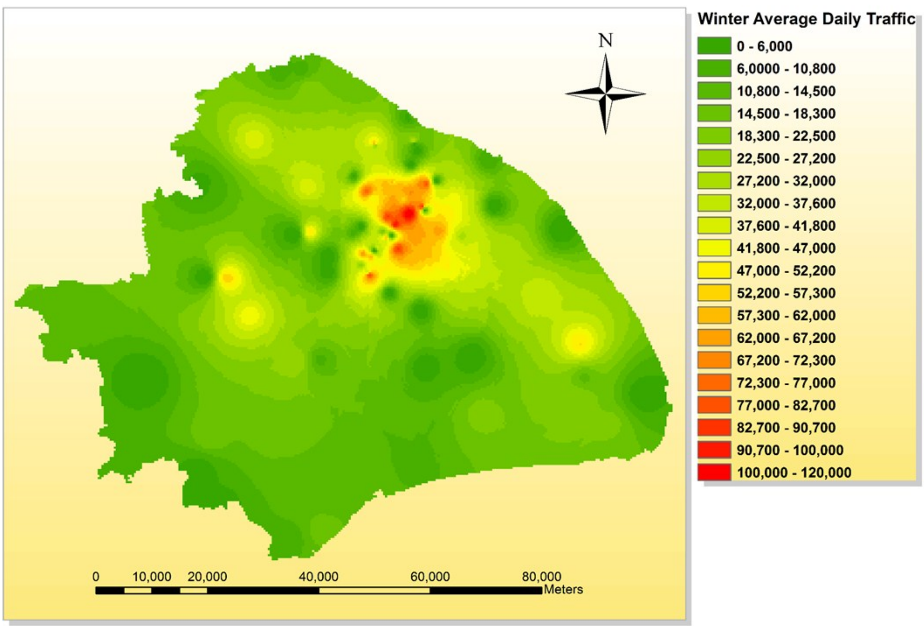

Fig. S6 GIS maps of average winter traffic volumes in Shanghai. (Data source: Shanghai Road Administration Bureau. According to data from 84 traffic volume monitoring points near our sampling sites)

7. Principal component analysis (PCA)

PCA was performed using SPSS software following a varimax rotation method for the source apportionment of metals in the aerosolized dust samples. Data from site 5 was not included due to the elevated Pb contamination in that sample. As presented in Table S3, four components were identified. PC1 had the highest loading: Fe, Mn, Co and Ni explaining 25.7% of the variance. Fe, Mn, Co and Ni were found to be originating mainly from the steel industry and automobile manufacturing industry, which are widely distributed in the Baoshan, Jiading, and Jinshan districts in Shanghai. PC2 explained 21.9% of the variance and was related to V, As, Mo and Sn, indicating mixed sources as these metals are used in various industries. PC3 was linked to Zn, Cd, Ba and Pb, explaining 20.6% of the variance and indicating vehicle emissions as a significant source. Pb is an indicator of vehicle exhaust pollution, Cd might be related to fossil fuel burnings, and Zn and Ba are typical contaminants originating from vehicular brake wear. PC4 was related to Cr and Cu, explaining 11.5% of the variance. Cu is used as a main raw material in various products, thus it could come from the manufacturing industry, which is mainly located in the Jinshan district.

Table S3 Results of principal component analysis carried out for source apportionment of metals in sampling sites.

	PC1	PC2	PC3	PC4
V	-0.00	**0.95**	-0.12	-0.08
Cr	0.53	0.28	0.14	**0.69**
Fe	**0.76**	0.04	0.47	0.11
Mn	**0.89**	0.01	0.25	-0.05
Co	**0.82**	0.05	0.08	-0.09
Ni	**0.65**	0.38	0.31	0.32
Cu	-0.23	-0.20	-0.04	**0.89**
Zn	0.23	-0.13	**0.84**	0.15
As	-0.09	**0.92**	0.03	-0.10
Mo	0.59	**0.70**	-0.04	-0.05
Cd	-0.12	0.08	**0.67**	-0.23
Sn	0.42	**0.74**	-0.03	0.34
Ba	0.35	-0.07	**0.80**	0.08
Pb	0.32	-0.04	**0.82**	0.08
Eigenvalues	3.60	3.07	2.88	1.61
Percentage of vanance explained (%)	25.7	21.9	20.6	11.5

8. Relationship between metal concentrations in aerosolized and bulk dust samples

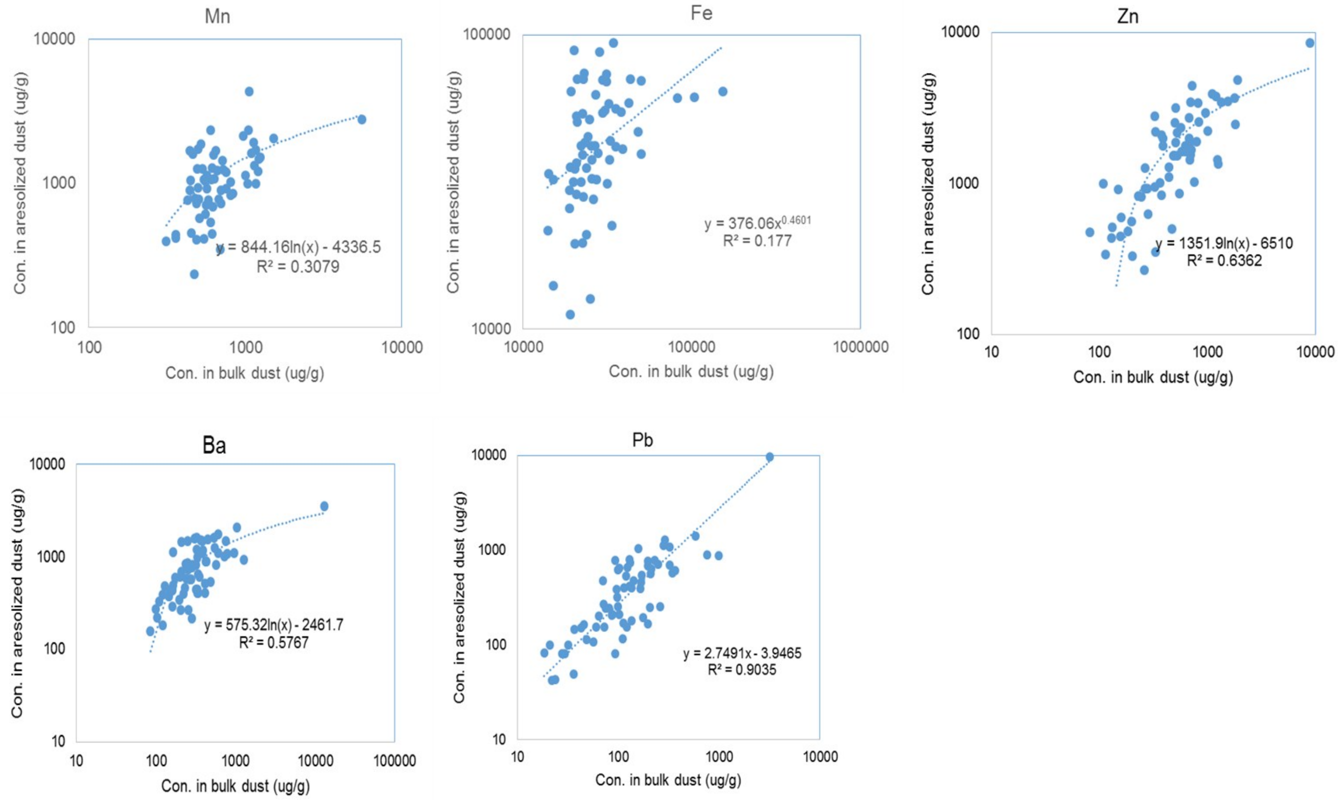

Fig. S7 Correlation between metal concentrations in aerosolized and bulk dust samples

9. Electron microscopy imaging of aerosolized dust samples

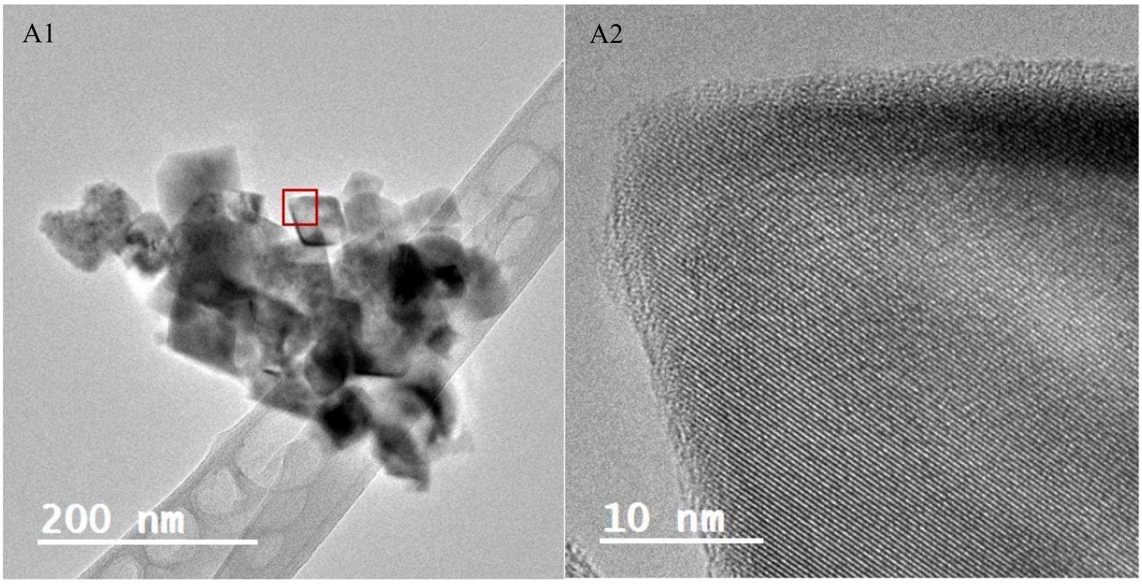

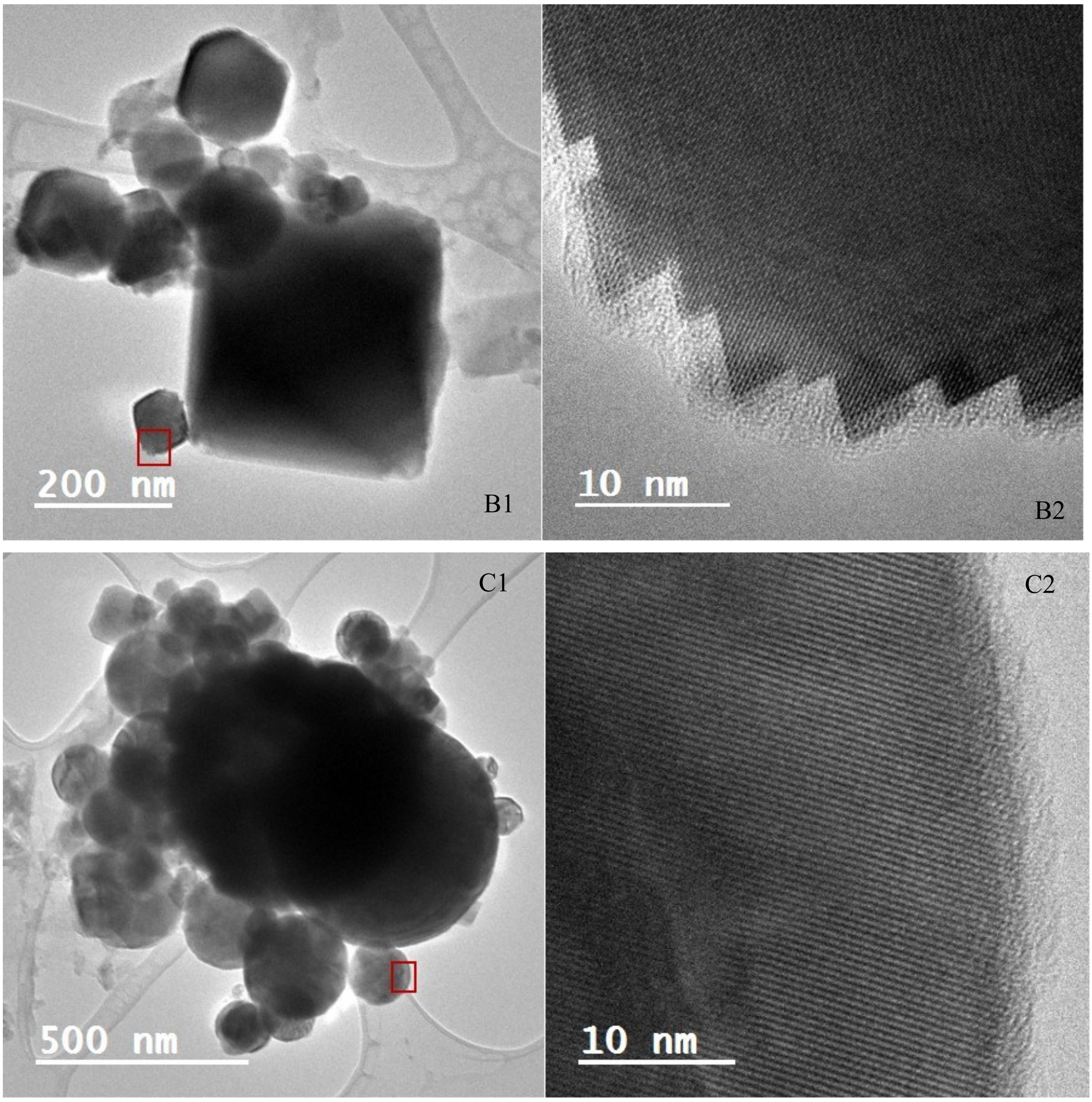

Fig. S8 Magnetite particles (A1-C1) with various morphologies and primary sizes found in dust samples and A2-C2 are the magnified image of the selected area in A1-C1, showing the lattice fringe of planes (2 2 0) and (1 1 1). A1 shows an aggregate of magnetite NPs with sizes ranging from 30 to 80 nm; B1 shows a magnetite particle with a clear octahedral shape of about 400 nm aggregated with small particles in the size of 40-150 nm. C1: These spherical magnetite are large particles (500-600 nm) surrounded by small spherules (50-200nm).

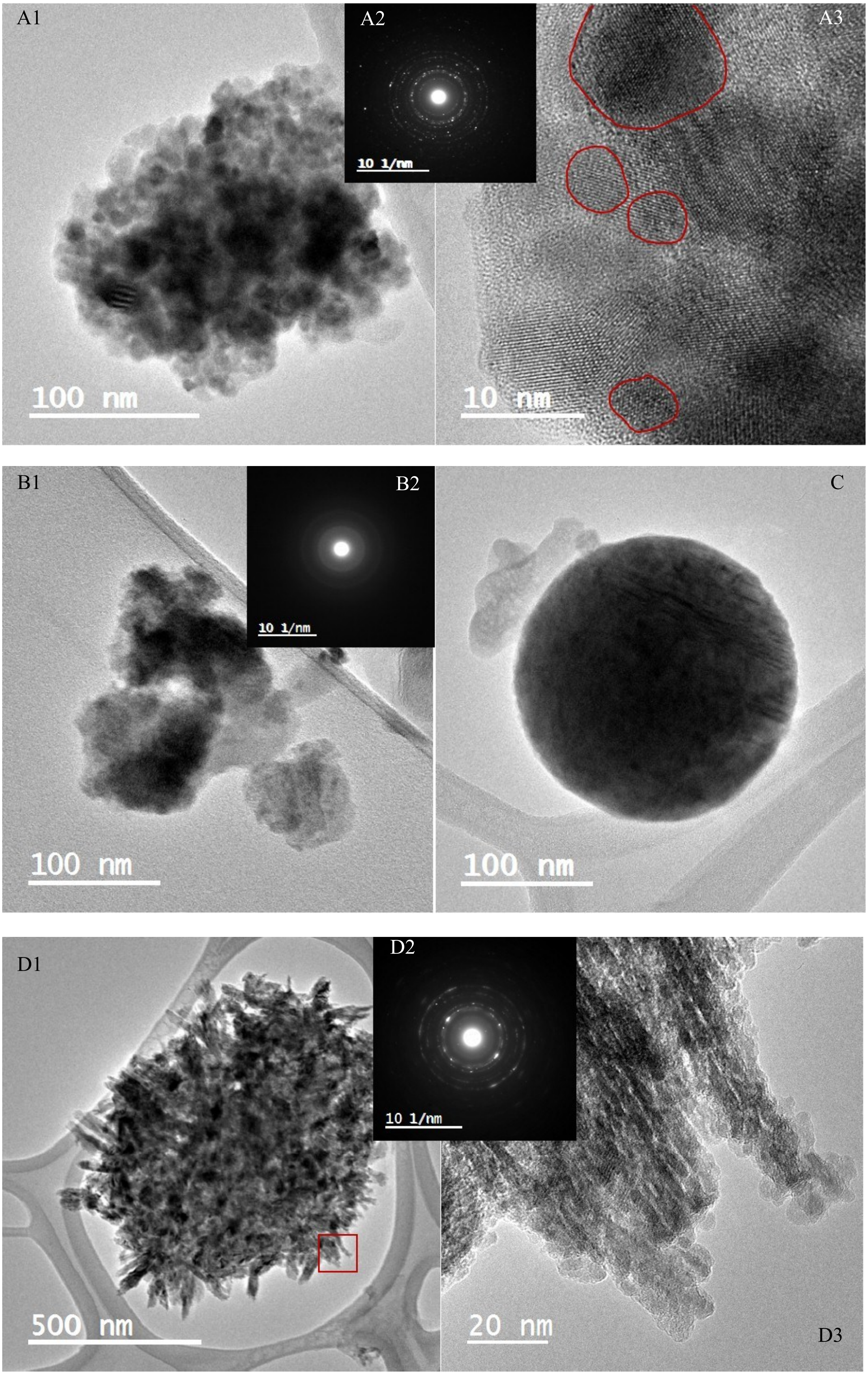

Fig. S9 Iron NPs, including hematite (A), ferrihydrite (B), Fe-riched fly ash (C) and goethite (D) identified in aerosolized dust samples. A2, B2 and D2 are the corresponding SAED images for NPs shown in A1, B1 and D1, respectively, and A3 and D3 are the magnified images of selected areas in A1 and D1.

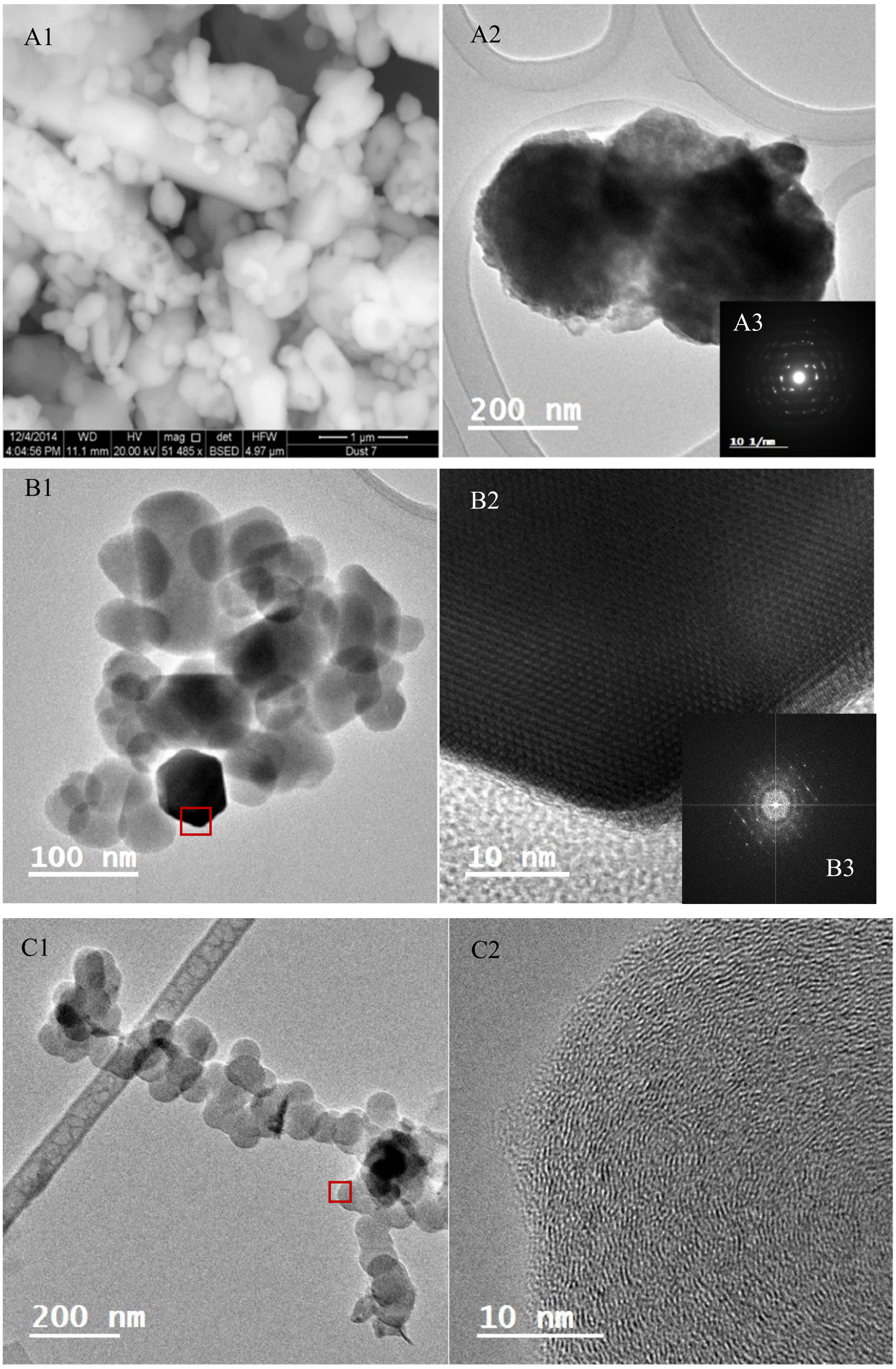

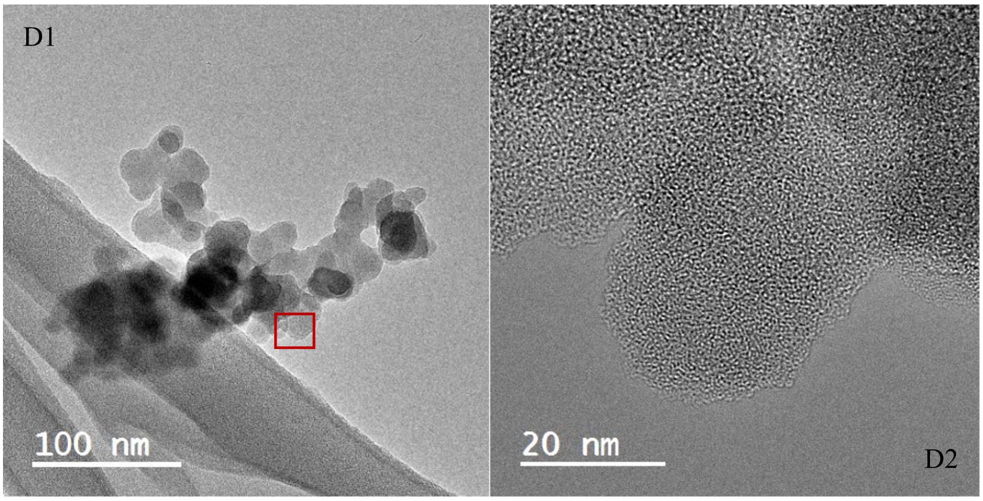

Fig. S10 Other typical NPs, including barite (A), hydroxyapatite (B), soot (C) and amorphous silica (D) found in aerosolized dust samples. B2-D2 are the magnified image of the selected area in B1-D1. A3 is the SAED of a single particle in A2; B3 is the corresponding FFT image of B2.

10. Aerosol characteristics, emission factors, and enrichment factors

Table S4. Aerosol characteristics and emission factors (average ± standard error).

Sampling site	Median aerosol size (nm)	Primary peak aerosol size (nm)	Second peak aerosol size (nm)	Aerosol emission factor (particles per mg dust)	Aerosol mass emission factor (µg aerosol per mg dust)
5	29.8	28.4	897.7	$(7.2 \pm 0.2)\times10^6$	0.78 ± 0.05
7	39.0	35.2	1036.6	$(4.3 \pm 0.3)\times10^7$	4.80 ± 0.09
9	779.8	264.2	ND	$(3.3 \pm 0.1)\times10^6$	0.82 ± 0.03
13	47.7	40.7	897.7	$(2.0 \pm 0.1)\times10^7$	2.52 ± 0.02
26	36.8	32.8	964.7	$(2.9 \pm 0.2)\times10^7$	3.60 ± 0.09
35	140.8	28.4	897.7	$(1.1 \pm 0.4)\times10^7$	1.77 ± 0.27
42	402.0	378.6	ND	$(1.9 \pm 0.3)\times10^7$	6.68 ± 0.56
47	41.3	37.9	1114.0	$4.7\times10^{7*}$	6.80*
48	45.1	37.9	673.2	$(4.1 \pm 0.3)\times10^6$	0.85 ± 0.04
51	445.9	406.8	ND	$(6 \pm 2)\times10^6$	4.06 ± 0.60
53	39.2	35.2	964.7	$1.6\times10^{7*}$	1.94*
66	39.4	32.8	777.4	$2.2\times10^{7*}$	3.17*
Average	*174 ± 73*	*133 ± 44*	*914 ± 46*	$(1.9 \pm 0.4)\times10^7$	*3.2 ± 0.7*

ND: Unimodal distribution; no secondary peak detected.

* Only one sample was aerosolized due to insufficient sample mass for replicates.

Table S5. Aerosol enrichment factors, a ratio of metal concentrations in aerosol over bulk dust samples.

Sampling site	**Average aerosol enrichment factor (*ef*)**
5	$(1.5 \pm 0.7)\times10^4$
7	$(1.4 \pm 1.2)\times10^3$
9	$(4.8 \pm 2.2)\times10^3$
13	$(4.8 \pm 1.9)\times10^3$
26	$(1.1 \pm 0.6)\times10^4$
35	$(2.5 \pm 1.4)\times10^4$
42	$(1.4 \pm 0.9)\times10^4$
47	$(1.3 \pm 0.7)\times10^4$
48	$(1.1 \pm 0.6)\times10^4$
51	$(1.2 \pm 0.6)\times10^4$
53	$(8.5 \pm 3.7)\times10^3$
66	$(8.9 \pm 4.0)\times10^3$